Journal of Materials Chemistry A

Accepted Manuscript

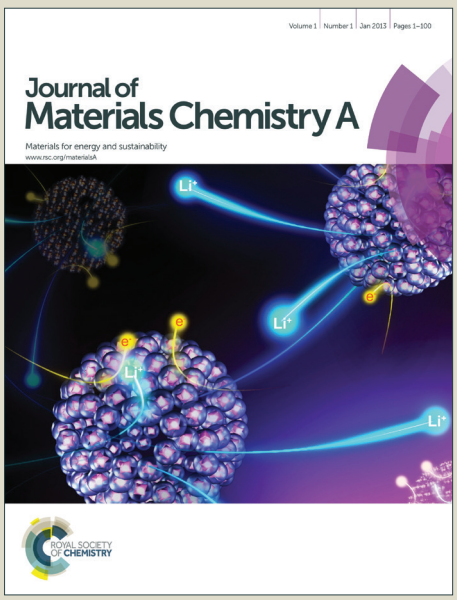

ROYAL SOCIETY OF CHEMISTRY

www.rsc.org/materialsA

Journal Name

RSCPublishing

ARTICLE

Synthesis of 6*H*-benzo[c]chromene as a new electron-rich building block of conjugated alternating copolymers and its application to polymer solar cells†

Right column;Cite this: DOI: 10.1039/x0xx00000x

Jong Won Lee, Seunghwan Bae and Won Ho Jo*

Received 00th January 2012,
Accepted 00th January 2012

DOI: 10.1039/x0xx00000x

www.rsc.org/

For the purpose to reduce the bandgap of fluorene-based semiconducting polymer, we introduced strong electron-donating oxygen atom into fluorene (F) to synthesize benzochromene (BC), which was then polymerized with electron deficient dithienyl benzothiadiazole (DTBT) and diketopyrrolopyrrole (DPP2T) to afford two low-bandgap polymers, PBCDTBT and PBCDPP2T, respectively. The PBCDTBT-based solar cell exhibits a promising power conversion efficiency (PCE) of 5.74%, which is much higher than that of the reference polymer (PFDTBT) (2.56%). The higher PCEs of BC-based polymers are mainly attributed to higher J_{SC}, which arises from stronger and broader absorption, higher exciton generation rate, more effective charge separation and higher hole mobility as compared to fluorine-based polymers.

Introduction

Bulk heterojunction (BHJ) polymer solar cells (PSCs) composed of conjugated copolymer as donor and fullerene derivative as acceptor have extensively been studied for the past decade because of their unique advantages such as low cost, light weight and flexibility.[1–5] Recently, remarkable progress has been made in polymer/fullerene BHJ solar cells, demonstrating that the power conversion efficiency (PCE) of PSCs reaches over 8 %.[6–11] However, it is still needed to further improve the PSC performance for commercialization. One of the most effective methods to improve the PCE is to develop new donor polymers, which have ideal energy levels and planar structure as well as good solubility in organic solvents.

To obtain high short-circuit current (J_{SC}) of PSCs, one must consider several factors: (i) broad and strong light absorption in the active layer,[12–16] (ii) efficient charge separation before geminate recombination[17–20] and (iii) good charge transport characteristics[21–24] of conjugated copolymers. A commonly used strategy to acquire broad and strong absorption in the active layer is to synthesize low bandgap polymer, consisting of alternating electron-donating and electron-accepting units. It has been known that the charge separation is dependent upon the dipole moment change of donor polymer from the ground state to the excited state ($\Delta\mu_{ge}$).[17–20] As proposed by Yu[17,18] and other groups,[19,20] a large value of $\Delta\mu_{ge}$ suppresses geminate recombination and facilitates charge separation. Another approach to improve J_{SC} is to incorporate planar molecular unit in polymer backbone, which may enhance electron delocalization and promote cofacial π–π stacking, thus benefitting charge transport in PSC device. To precisely control the highest occupied molecular orbital (HOMO) energy level of donor polymer and thus to improve the open-circuit voltage (V_{OC}) of PSCs,[25,26] alternating conjugated copolymers composed of weak electron-donating and strong electron-accepting units have been developed.[27–33]

Among various semiconducting polymers for PSCs, a copolymer consisting of fluorine as electron-donating unit and benzothiadiazole as an electron-accepting unit, poly{9,9-bis-alkylfluorene-2,7-diyl-alt-[4,7 bis-(thien-2-yl)-2,1,3-benzothia-diazole]-5′,5″-diyl} (PFDTBT), exhibits a high V_{OC} of around 1 V because of its deep HOMO energy level, but it shows relatively low PCEs with moderate J_{SC}s due to a large bandgap of 1.9 eV. The other critical issue of PFDTBT-based polymer is the solubility in organic solvent. Previously, it has been reported that bis-octyl-substituted PFDTBT has poor solubility, and therefore only low average molecular weight (M_n= ~5 k) of polymer was obtained, which leads to a low PCE of 2%.[34,35] Therefore, other PFDTBTs with longer and branched side chains such as decyl[36] (M_n=17 k), 2-ethylhexyl (M_n=21 k) and 3,7-dimethyloctyl[35] (M_n=20 k) were synthesized, and the devices based on these polymers showed higher PCEs of 4.0%–4.5% due to better solubility and higher molecular weight. However, the J_{SC}s of the devices are still moderate (7.0–9.0 mA/cm^2) probably because of large bandgap.

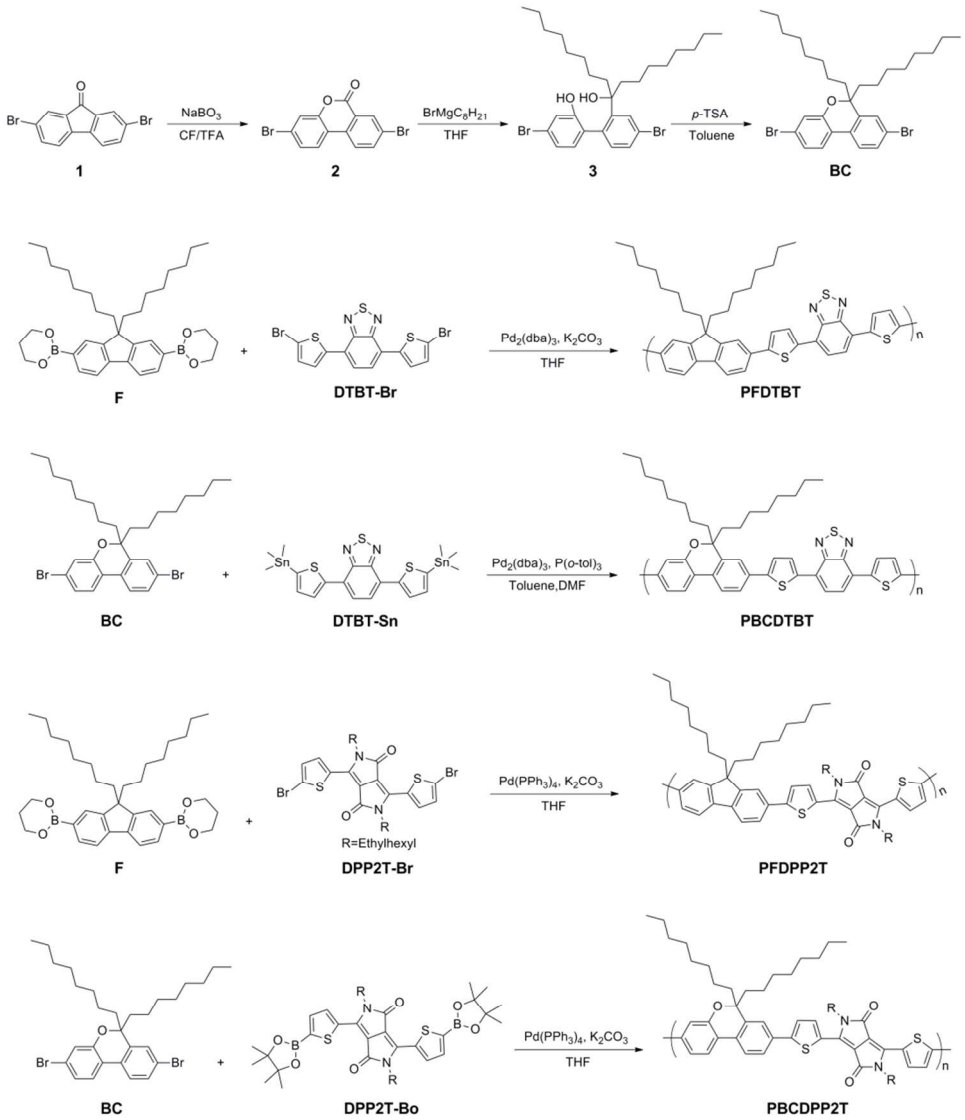

Scheme 1 Synthesis of monomer and polymers.

Another electron accepting unit that has attracted significant interest in the past few years is thiophene-capped diketopyrrolopyrrole (DPP2T), which exhibits intense absorption at long wavelength and good field effect mobilities.[12,22] Recently, Janssen group[37] synthesized a copolymer (PFDPP2T) consisting of DPP2T and fluorine, and utilized the copolymer in photovoltaic device. Although PFDPP2T-based device shows a high V_{OC} of ~0.9 V due to its deep HOMO energy level, the polymer affords a low PCE of 0.9% with a low J_{SC} of 2.41 mA/cm^2. One of the reasons for the low J_{SC} is probably a large bandgap of 1.79 eV, which is a common problem of fluorene-based polymer.

In this study, we introduce an oxygen atom into bis-octyl-substituted fluorene unit in order to develop a new electron-donating unit, benzochromene (BC). BC was then polymerized with an electron-accepting unit, dithienyl benzothiadiazole (DTBT) or DPP2T to synthesize two low bandgap polymers (PBCDTBT and PBCDPP2T) (see scheme 1). Since the electron-donating ability of BC is stronger than fluorene, it is expected that the BC-based polymers (PBCDTBT and PBCDPP2T) exhibit narrower bandgaps than the corresponding fluorine-based polymers (PFDTBT and PFDPP2T), respectively, by raising their HOMO energy level. BC-based polymers are also expected to have better solubility due to regio-random molecular structure in backbone and higher M_n than the corresponding fluorene-based polymer. The best device based on PBCDTBT exhibits a promising PCE of 5.74% with a J_{SC} of 12.51 mA/cm^2, which is two times higher than the J_{SC} of PFDTBT (6.35 mA/cm^2). The PBCDPP2T-based device also shows higher PCE (2.01%) with higher J_{SC} (5.79 mA/cm^2) than those of PFDPP2T-based device (PCE=0.95% and J_{SC} =2.79 mA/cm^2).

Results and discussion

Three polymers, PFDTBT, PFDPP2T and PBCDPP2T, were synthesized by the Suzuki coupling, and PBCDTBT was

Table 1 Characteristics of DTBT- and DPP-based polymers.

Polymer	M_n (kg/mol)	PDI	UV–Vis absorption		E_g^{opt} (eV)[a]	HOMO (eV)	LUMO (eV)[b]
			$\lambda_{max,\ CHCl3}$ (nm)	$\lambda_{max,\ film}$ (nm)			
PFDTBT	19.0	2.6	384, 542	386, 555	1.81	–5.43	–3.62
PBCDTBT	46.0	2.2	406, 594	409, 570	1.77	–5.28	–3.51
PFDPP2T	12.4	2.1	604, 654	601, 652	1.73	–5.55	–3.82
PBCDPP2T	18.6	1.9	642, 687	631, 685	1.64	–5.31	–3.67

[a]Determined from the onset of UV–Vis absorption spectra. [b]Calculated from LUMO=HOMO+E_g^{opt}.

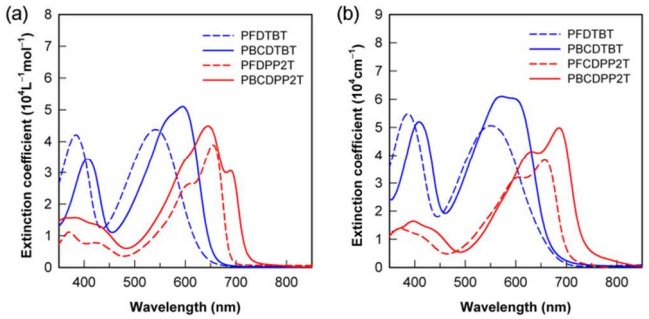

Fig. 1 UV–Vis absorption spectra of polymers in chloroform solution (a) and in film (b).

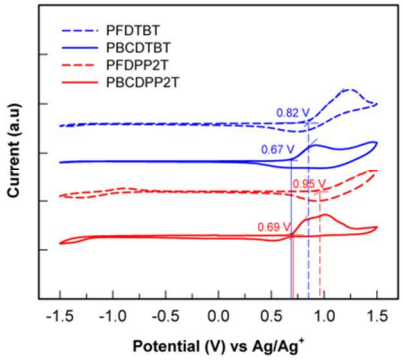

Fig. 2 Cyclic voltammograms of polymers.

synthesized by Stille coupling reaction. The M_ns of PFDTBT and PFDPP2T are 19.0 and 12.4 kDa with polydispersity indexes of 2.6 and 2.1, respectively, while PBCDTBT and PBCDPP2T have the M_n of 46.0 and 18.6 kDa with polydispersity indexes of 2.2 and 1.9, respectively, as measured by gel permeation chromatography (Table 1).

When the UV–Visible spectra of PFDTBT and PBCDTBT are compared, as shown in Figure 1a, PBCDTBT absorbs more photons in the range of 550–700 nm with higher molar extinction coefficient (ε_{max}) than PFDTBT. Furthermore, PBCDTBT exhibits strong vibronic shoulder in solution, indicating that PBCDTBT is significantly aggregated in the solution state. When the UV–Visible spectra of two polymers in film state are compared, as shown in Figure 1b, it also reveals that PBCDTBT exhibits higher ε_{max} and broader absorption than PFDTBT. Thus, it is easily expected that more excitons are generated in PBCDTBT than in PFDTBT when they are exposed to the light. Since strong vibronic shoulder appears in the film of PBCDTBT while PFDTBT film does not exhibit the vibronic shoulder, it is concluded that PBCDTBT has more ordered structure than PFDTBT in solid state. When the optical bandgap (E_g^{opt}) of PBCDTBT is estimated from the absorption edge of thin film, the E_g^{opt} of PBCDTBT (1.77 eV) is slightly lower than that of PFDTBT (1.81 eV). The two absorption bands of PBCDTBT are red-shifted in both solution and film state as compared to PFDTBT. PBCDPP2T also shows lower E_g^{opt} (1.64 eV) with higher ε_{max} than that of PFDPP2T (1.73 eV), because the electron-donating power of BC is stronger than fluorene.

When electrochemical properties of polymers are measured by cyclic voltammetry (CV), as shown in Figure 2, the HOMO energy levels of PBCDTBT (–5.28 eV) and PBCDPP2T (–5.31 eV) are higher than those of PFDTBT (–5.43 eV) and PFDPP2T (–5.55 eV), respectively. This is easily understood because the electron-donating power of BC in PBCDTBT and PBCDPP2T is stronger than that of fluorene in PFDTBT and PFDPP2T. It should be noted here that the strong electron-donating unit in a donor polymer raises the HOMO energy level. Since the LUMO energy levels of PFDTBT, PBCDTBT, PFDPP2T and PBCDPP2T are –3.62 eV, –3.51 eV, –3.82 eV and –3.67 eV, respectively, as listed in Table 1, the LUMO–LUMO offsets between the donor polymers and $PC_{71}BM$ (–4.2 eV) are larger than 0.3 eV, which are sufficient for effective exciton dissociation.[38,39]

When the solar cell performances are measured with the conventional device structure, as shown in Figure 3a, the best device based on PBCDTBT exhibits a promising PCE of 5.74% with a J_{SC} of 12.51 mA/cm^2, a V_{OC} of 0.87 V and a FF of 52% while the PFDTBT shows a PCE of 2.56% with a J_{SC} of 6.35 mA/cm^2, a V_{OC} of 0.94 V and a FF of 43%. Another BC-based polymer, PBCDPP2T, also shows higher PCE (2.01%) than that of fluorene-based counterpart, PFDPP2T (0.95%). Here, the devices with fluorine-based polymers were optimized by following the method reported in the literatures[35,37] while the devices with BC-based polymers were optimized by varying the blend ratio of polymer to $PC_{71}BM$, the mixing ratio of solvents and the amount of DIO additive. Since the V_{OC} is proportional to the energy difference between the LUMO energy level of $PC_{71}BM$ and the HOMO energy level of donor polymer, it is reasonable that the V_{OC}s of PFDTBT (0.94 V) and PFDPP2T (0.91 V) are higher than those of PBCDTBT and PBCDPP2T, respectively, considering that the HOMO energy levels of

Table 2 Photovoltaic properties of devices under standard AM 1.5G illumination and charge carrier mobilities under dark condition.

Polymers	Polymers:$PC_{71}BM$ (w/w)	Thickness (nm)	V_{OC} (V)	J_{SC} (mA/cm^2)	FF	μ_h (cm^2/V s)[a]	μ_h (cm^2/V s)[b]	PCE (%)
PFDTBT	1:4	80±5	0.94±0.01	6.26±0.11	0.40±0.02	$(5.0\pm0.3)\times10^{-4}$	$(0.9\pm0.3)\times10^{-4}$	2.41±0.07
PBCDTBT	1:1.5	77±5	0.86±0.01	12.48±0.20	0.51±0.01	$(1.0\pm0.1)\times10^{-3}$	$(5.2\pm0.5)\times10^{-4}$	5.56±0.14
PFDPP2T	1:4	75±5	0.91±0.01	2.64±0.15	0.34±0.01	$(7.4\pm0.2)\times10^{-6}$	$(4.4\pm0.3)\times10^{-6}$	0.85±0.08
PBCDPP2T	1:3	70±5	0.78±0.02	5.58±0.19	0.42±0.02	$(2.0\pm0.1)\times10^{-5}$	$(8.7\pm0.3)\times10^{-6}$	1.85±0.12

[a]Hole mobility in pristine polymer as measured by SCLC method. [b]Hole mobility in the blend of polymer:$PC_{71}BM$ as measured by SCLC method.

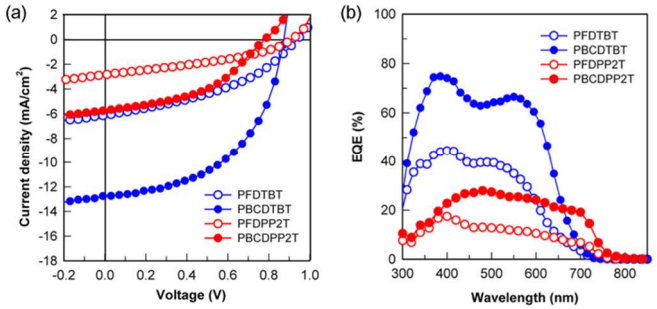

Fig. 3 *J*–*V* curves of polymer/$PC_{71}BM$ BHJ solar cells under AM 1.5G, 100 mW/cm^2 (a) and external quantum efficiency spectra of polymer/$PC_{71}BM$ solar cells (b).

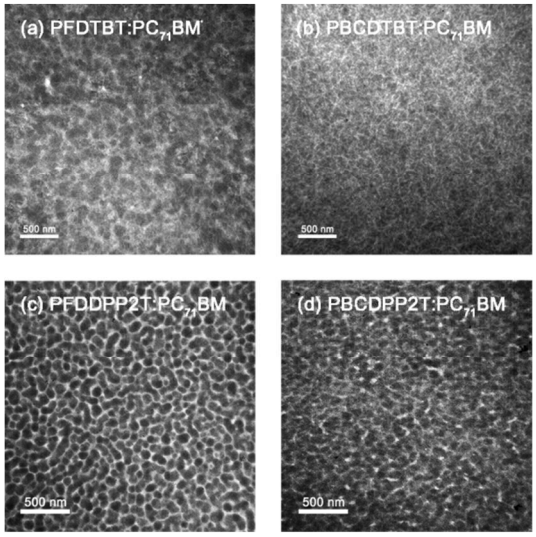

Fig. 4 TEM images of polymers/$PC_{71}BM$ blend films

fluorene-based polymers are deeper than those of BC-based polymers. Although the V_{OC} is sacrificed to some extent upon introduction of oxygen in fluorene unit, the J_{SC}s of PBCDTBT (12.51 mA/cm^2) and PBCDPP2T (5.79 mA/cm^2) are two times larger than those of PFDTBT (6.35 mA/cm^2) and PFDPP2T (2.84 mA/cm^2), respectively, which can be further identified by comparing the external quantum efficiencies (EQE) of the four polymers as blended with $PC_{71}BM$ (Figure 3b). Integration of EQE spectra of PFDTBT, PBCDTBT, PFDPP2T and PBCDPP2T blends yields J_{SC}=6.11 mA/cm^2, J_{SC}=11.86 mA/cm^2, J_{SC}=2.61 mA/cm^2 and J_{SC}=5.49 mA/cm^2, respectively, which are nearly consistent with the J_{SC} values obtained from *J*–*V* measurement.

Three factors may be considered for higher J_{SC} of BC-based polymer solar cell: molecular weight, UV–Vis absorption and blend morphology. First, high molecular weight of donor polymer is beneficial for effective charge transport, because it may facilitate formation of bicontinuous phase structure.[40] To examine the effect of molecular weight on photovoltaic properties, we synthesized two PFDTBTs with different molecular weights (8.3 and 19.0 k) and compared their solar cell performances. The best device based on PFDTBT with M_n=19.0 k shows a PCE of 2.56% with J_{SC}=6.35 mA/cm^2, V_{OC}=0.94 V and FF=0.43, while the device based on lower molecular weight PFDTBT (M_n=8.3 k) exhibits a PCE of 2.29% with J_{SC}=6.11 mA/cm^2, V_{OC}=0.94 V and FF=0.40 (Figure S3), indicating that the molecular weight does not strongly affect the photovoltaic properties when the molecular weight exceeds 8.3 k. It has also been reported that the photovoltaic properties of PFDTBT are saturated when M_n>10 k.[41] Second, strong and broad light absorption is also an important factor for achieving high J_{SC}. The stronger and broader light absorption of PBCDTBT and PBCDPP2T contributes to larger J_{SC} than PFDTBT and PFDPP2T, respectively (Figure 1). Third, the morphology of polymer:PCBM blend is also a critical factor to control J_{SC}. Since the transmission electron microscopy (TEM) images of BC-based polymer blends exhibit nanoscale phase separation with fibril-like network structure while fluorine-based polymer blends show coarser morphology with larger domain sizes (Figure 4), it is expected that the BC-based polymer blends are more effective for both charge separation and charge transport.[42]

To analyze the effect of oxygen atom in PBCDTBT and PBCDPP2T on PSC device performance in more detail, we determined the maximum exciton generation rate (G_{max}) and exciton dissociation probability ($P(E,T)$) of the four polymers according to the method previously reported,[43,44] and compared them with each other. Figure 5a shows the dependence of photocurrent density (J_{ph}) on effective voltage (V_{eff}). Here J_{ph} is defined as $J_{ph}=J_L-J_D$, where J_L and J_D are the current density under illumination at 100 mW/cm^2 and dark condition, respectively, and V_{eff} is defined as $V_{eff}=V_0-V_a$, where V_0 is the voltage at the point of J_{ph}=0 and V_a is the applied bias voltage. Since it can be assured that all of photogenerated excitons are dissociated into free charge carriers at high V_{eff} due to sufficient electric field,[45] the G_{max} can be determined from the saturation current density

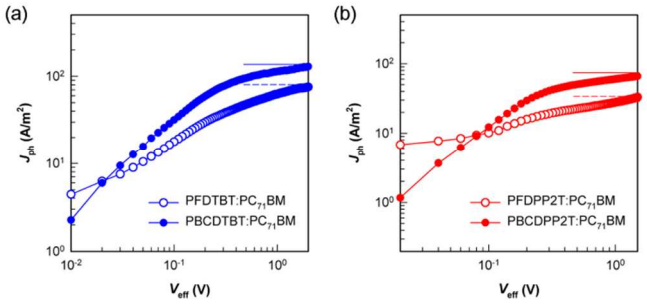

Fig. 5 Photocurrent density (J_{ph}) plotted against effective voltage (V_{eff}) under optimized condition.

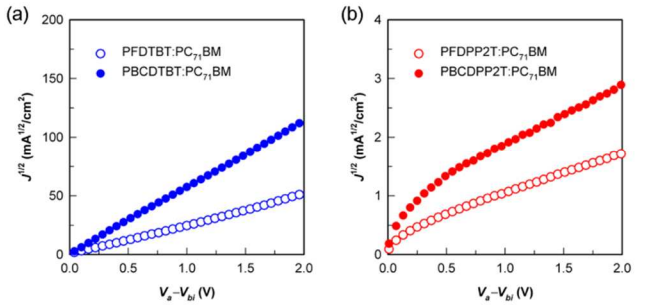

Fig. 6 Dark *J*–*V* characteristics of polymers:PC$_{71}$BM blends with hole-only device.

(J_{sat}): $J_{sat}=qG_{max}L$, where q is the electronic charge and L is the thickness of active layer. When the value of G_{max} is calculated from the above relation and Figure 5a, the value of G_{max} for PBCDTBT (8.55×10^{27} /m^3 s with J_{sat}=115 A/m^2) is larger than that of PFDTBT (5.66×10^{27} /m^3 s with J_{sat}=77 A/m^2). This is probably because PBCDTBT shows higher ε_{max} and broader absorption than PFDTBT. The exciton dissociation probability ($P(E,T)$), which is a function of the electric field (E) and temperature (T), can also be determined from the relation $J_{ph}=qG_{max}P(E,T)L$. Figure S5a shows a plot of $P(E,T)$ against V_{eff}, where the dashed-line indicates V_{eff} and the corresponding $P(E,T)$ under short-circuit condition. The $P(E,T)$ values of PFDTBT and PBCDTBT under short-circuit condition are 79% and 85%, respectively, suggesting that excitons photogenerated in PBCDTBT dissociate more efficiently than those in PFDTBT. DPP-based polymer shows the same result as BT-based polymer, as shown in Figure 5b and Figure S5b: PBCDPP2T exhibits larger G_{max} (5.89×10^{27} /m^{3}s) and higher $P(E,T)$ (82%) than those of fluorene-based counterpart, PFDPP2T (2.42×10^{27} /m^{3}s and 75%).

It has been reported that the difference between the dipole moment from ground state to excited state ($\Delta\mu_{ge}$) in conjugated polymers largely affects the device performance of PSCs.[17–20] Since a large value of $\Delta\mu_{ge}$ in donor polymer makes the excited state highly polarized, it facilitates electron transfer from donor polymer to acceptor. In other words, Coulombic binding energy of exciton is reduced by larger $\Delta\mu_{ge}$. When the $\Delta\mu_{ge}$ was calculated for one repeating unit of the four polymers using DFT/TDDFT at B3LYP/6-31G level, the $\Delta\mu_{ge}$ of BC-based polymers are larger than the corresponding fluorene-based polymers (see Table S4 and Table S5), indicating that excitons in BC-based polymers are more easily separated into free charge carriers than fluorine-based polymers, which is very consistent with the value of $P(E,T)$.

Another important factor to control J_{SC} is the crystallinity of donor polymer, because high crystalline polymer affords efficient charge carrier transport to electrode after exciton dissociation. When the crystallinities of two polymers are examined by wide angle X-ray diffraction (XRD), as shown in Figure S6, the XRD patterns of BC-based two polymers clearly show distinctive Bragg diffraction, while those of fluorine-based polymers do not show a discernible peak,[46] indicating that BC-based polymers are highly crystalline whereas fluorine-based polymers are amorphous. To investigate the molecular orientation of the polymers blended with PC$_{71}$BM, the grazing incident wide angle X-ray scattering (GIWAXS) experiments are performed. The PBCDTBT:PC$_{71}$BM blend clearly shows (100), (200), (300) and (010) diffraction peaks in q_z direction, while the diffraction peaks of (100) and (200) are also observed in q_{xy} direction, indicating that PBCDTBT has both face-on and edge-on molecular orientation on the substrate. However, the PFDTBT:PC$_{71}$BM blend does not exhibit discernible diffraction peaks in both q_z and q_{xy} direction, indicating amorphous characteristic (Figure S7).

To correlate crystallinity to charge transport, the hole mobilities of the four polymers and their blends with PC$_{71}$BM are measured by the standard method using a single charge carrier device and compared with each other. The space-charge limited current (SCLC) *J*–*V* curves were obtained under dark condition using hole-only device (ITO/PEDOT:PSS/polymer or polymer:PC$_{71}$BM/Au), from which the hole mobility was calculated using the Mott-Gurney law (Figure 6, Table 2 and Figure S8). When the hole mobilities of BC-based polymers and their blends with PC$_{71}$BM are compared with those of fluorine-based polymers and their blends with PC$_{71}$BM, the hole mobilities of BC-based polymers and their blends are higher than those of fluorine-based polymers and their blends, respectively. Considering that BC-based polymers, PBCDTBT and PBCDPP2T, have higher crystallinity than fluorene-based polymers, PFDTBT and PFDPP2T, the higher hole mobilities of BC-based polymers are attributed to higher crystallinity as compared to fluorene-based polymers. In short, higher J_{SC}s of BC-based polymers arise from larger photon absorption, higher G_{max}, more effective charge separation, higher hole mobility and better developed morphology as compared to fluorine-based polymers.

Conclusions

We synthesized a new electron-donating unit, BC, by introducing an oxygen atom into fluorene, which was then polymerized with electron-deficient DTBT and DPP2T, for the purpose of reducing the bandgap and enhancing the solubility of conjugated polymer. The bandgaps of BC-based polymers, PBCDTBT and PBCDPP2T, are lower than those of fluorine-based counterparts, PFDTBT and PFDPP2T, respectively, due to the introduction of electronegative oxygen atom in fluorene.

Since BC-based polymers exhibit stronger and broader light absorption, higher exciton generation rate as evidenced by larger G_{max}, more effective charge generation rate due to larger $\Delta\mu_{ge}$ and higher mobility due to higher crystallinity than the corresponding fluorine-based counterparts, BC-based polymers show higher J_{SC} than fluorine-based polymers. Particularly, the PSC based on PBCDTBT:$PC_{71}BM$ shows a promising PCE of 5.74% with a J_{SC} of 12.51 mA/cm^2, a V_{OC} of 0.87 V and FF of 52%.

Experimental

Materials

4,7-bis(5-bromothiophen-2-yl)benzo[c][1,2,5]thiadiazole (**DTBT-Br**), 4,7-bis(5-(trimethylstannyl)thiophen-2-yl)benzo-[c][1,2,5]thiadiazole (**DTBT-Sn**), 3,6-bis(5-bromothiophen-2-yl)-2,5-bis(2-ethylhexyl)pyrrolo[3,4-c]pyrrole-1,4(2*H*,5*H*)-dione (**DPP2T-Br**) and 2,5-bis(2-ethylhexyl)-3,6-bis(5-(4,4,5,5-tetramethyl-1,3,2-dioxaborolan-2-yl)thiophen-2-yl)pyrrolo[3,4-c]pyrrole-1,4(2*H*,5*H*)-dione (**DPP2T-Bo**) were synthesized by following the methods reported in literature.[47,48] 9,9-Dioctylfluorene-2,7-diboronic acid bis(1,3-propanediol) ester (**F**), 2,7-Dibromo-9-fluorenone, sodium perborate monohydrate, octylmagnesium bromide, *p*-toluenesulfonic acid monohydrate, 2,2,6,6-tetramethylpiperdine, *n*-butyllithium and trimethyltin chloride were purchased from Sigma-Aldrich and used without further purification. [6,6]-Phenyl-C_{71}-butyric acid methyl ester ($PC_{71}BM$) was obtained from Nano-C. Poly(3,4-ethylenedioxy-thiophene):poly(styrene sulfonate) (PEDOT:PSS) (Clevious P VP AI 4083) was purchased from H. C. Stark and passed through a 0.45 μm PVDF syringe filter before spin-coating. Common organic solvents were purchased from Daejung. Tetrahydrofuran (THF) was dried over sodium/benzophenone under nitrogen condition and freshly distilled prior to use. All other reagents were purchased from Tokyo Chemical Industry and used as received.

Synthesis of 3, 8-dibromo-6*H*-benzo[c]chromen-6-one (2)

The compound **1** (1.00 g, 2.96 mmol) was dissolved in a mixed solvent of 15 mL of chloroform and 15 mL of trifluoroacetic acid, followed by addition of sodium perborate monohydrate (0.68 g, 6.80 mmol) in one portion. After the reaction mixture was stirred at room temperature for 12 h, it was poured into 150 mL of dichloromethane and then extracted with water, sodium bicarbonate and brine. The organic phase was collected and dried over $MgSO_4$. The product was sequentially recrystallized with toluene and then chloroform to afford light yellow powder (1.69 mmol, 56%). ^{1}H NMR (300 MHz, $CDCl_3$): δ□(ppm) 8.49 (s, 1H), 7.92 (s, 2H), 7.85 (d, 1H), 7.51 (d, 1H), 7.48–7.44 (m, 1H). ^{13}C NMR (125 MHz, $CDCl_3$): δ (ppm) 159.19, 151.38, 138.18, 133.35, 132.89, 128.15, 124.23, 123.86, 123.41, 123.21, 122.48, 121.08, 116.44. HRMS (EI, *m*/*z*): Calculated for $C_{13}H_6Br_2O_2$: 351.87, found: 351.87.

Synthesis of 4, 4'-dibromo-2'-(9-hydroxyheptadecan-9-yl)-[1, 1'-biphenyl]-2-ol (3)

The compound **2** (0.50 g, 1.41 mmol) was dissolved in dry THF (20 mL) under argon and kept at 0 °C. 1 M diethyl ether solution of octylmagnesium bromide (3.26 mL, 3.26 mmol) was slowly added into the solution. The resulting solution was then warmed to room temperature and stirred for 10 h. The reaction mixture was quenched by addition of 12 mL of water and 3 mL of hydrochloric acid, and then extracted with DCM. After the organic phase was dried over $MgSO_4$, the solvent was evaporated under reduced pressure. The crude product was purified by column chromatography on silica gel using ethyl acetate and hexane mixture (1:8, v:v) as an eluent to obtain light yellow oil (1.06 mmol, 75%). ^{1}H NMR (300 MHz, $CDCl_3$): δ (ppm) 7.66 (d, 1H), 7.42 (m, 1H), 7.13 (d, 1H), 7.07 (m, 1H), 6.84–6.91 (m, 2H), 5.29 (s, 1H), 1.68 (s, 1H), 1.25–1.17 (m, 24H), 0.89–0.84 (m, 6H). ^{13}C NMR (125 MHz, $CDCl_3$): δ (ppm) 153.79, 147.20, 134.67, 132.58, 131.11, 130.88, 130.20, 129.33, 123.30, 122.98, 122.19, 119.67, 78.35, 42.19, 41.31, 31.83, 31.81, 30.32, 29.89, 29.72, 29.47, 29.37, 29.25, 29.18, 24.02, 23.47, 22.63, 22.61, 14.08. HRMS (EI, *m*/*z*): Calculated for $C_{29}H_{42}Br_2O_2$: 580.16, found: 580.15.

Synthesis of 3, 8-dibromo-6, 6-dioctyl-6*H*-benzo[c]chromene (BC)

The compound **3** (0.58 g, 1 mmol) was dissolved in toluene (20 mL) in a two-neck flask under argon. After *p*-toluenesulfonic acid monohydrate (0.57 g, 3 mmol) was added into the solution, the mixture was stirred at 120 °C for 15 h. The solution was cooled down to room temperature and extracted with DCM. After the organic phase was dried over $MgSO_4$, the solvent was evaporated under reduced pressure. The residue was purified by column chromatography on silica gel using hexane as an eluent to afford colorless oil (0.88 mmol, 88%). ^{1}H NMR (300 MHz, $CDCl_3$): δ (ppm) 7.53 (d, 1H), 7.48 (m, 1H), 7.41–7.44 (d, 1H), 7.20 (d, 1H), 7.10–7.07 (m, 2H), 1.83–1.81 (m, 4H), 1.29–1.21 (m, 24H), 0.88–0.83 (m, 6H). ^{13}C NMR (125 MHz, $CDCl_3$): δ (ppm) 153.68, 138.67, 130.64, 127.87, 127.67, 124.36, 123.74, 123.54, 122.76, 121.74, 120.92, 119.84, 82.99, 38.86, 31.81, 29.82, 29.36, 29.20, 23.54, 22.63, 14.08; HRMS (EI, *m*/*z*): Calculated for $C_{29}H_{40}Br_2O$: 562.14, found: 562.14.

Polymerization of PFDTBT

PFDTBT was synthesized by the Suzuki coupling. A mixture of **F** (0.15 g, 0.27 mmol), **DTBT-Br** (0.12 g, 0.27 mmol) and P(*o*-tol)$_3$ (0.02 g, 0.06 mmol) was dissolved in a mixture of aqueous K_3PO_4 solution (2 M, 3.3 mL) and THF (10 mL). After the solution was flushed with argon for 10 min, $Pd_2(dba)_3$ (0.02 g, 0.02 mmol) were added quickly in the reaction mixture and sealed. The reaction mixture was stirred at 140 ºC for 3 h in a microwave reactor. After being cooled to room temperature, the organic phase was poured into methanol during stirring. The precipitate was filtered through a Soxhlet thimble and subjected to Soxhlet extraction sequentially with methanol, acetone, ethyl acetate, hexane and chloroform. The polymer was recovered from the chloroform fraction, and precipitated into methanol to afford the product of reddish-purple solid (0.15 g, 69%). ^{1}H NMR (300 MHz, $CDCl_3$): δ (ppm) 8.13 (br, 1H), 7.89 (br, 1H),

7.66 (d, 3H), 7.46 (br, 1H), 7.34 (br, 2H), 2.04 (br, 3H), 1.11 (br, 16H), 0.78 (br, 8H).

Polymerization of PBCDTBT

PBCDTBT was synthesized by the Stille coupling. A mixture of **BC** (0.11 g, 0.19 mmol), **DTBT-Sn** (0.12 g, 0.19 mmol) and P(*o*-tol)$_3$ (0.01 g, 0.03mmol) was dissolved in mixture of toluene (9 mL) and DMF (1 mL). After the solution was flushed with argon for 10 min, $Pd_2(dba)_3$ (0.01 g, 0.01 mmol) was added quickly in the reaction mixture and sealed. The reaction mixture was stirred at 130 ºC for 2 h in a microwave reactor. After being cooled to room temperature, the organic phase was poured into methanol during stirring. The precipitate was filtered through a Soxhlet thimble and subjected to Soxhlet extraction sequentially with methanol, acetone, ethyl acetate, hexane and chloroform. The polymer was recovered from the chloroform fraction, and precipitated into methanol to afford the product of bluish-purple solid (0.07 g, 51%). ^{1}H NMR (300 MHz, $CDCl_3$): δ (ppm) 7.10 (br, 29H), 4.86 (br, 1H), 2.04 (br, 21H), 1.25 (br, 15H), 0.82 (br, 28H).

Polymerization of PFDPP2T

PFDPP2T was synthesized by the Suzuki coupling. A mixture of **F** (0.15 g, 0.27 mmol) and **DTBT-Br** (0.18 g, 0.27 mmol) was dissolved in a mixture of aqueous K_2CO_3 solution (2 M, 3.3 mL) and THF (10 mL). After the solution was flushed with argon for 10 min, $Pd(PPh_3)_4$ (0.02 g, 0.02 mmol) was added quickly in the reaction mixture and sealed. The reaction mixture was stirred at 140 ºC for 3 h in a microwave reactor. After being cooled to room temperature, the organic phase was poured into methanol under stirring. The precipitate was filtered through a Soxhlet thimble and subjected to Soxhlet extraction sequentially with methanol, acetone, ethyl acetate, hexane and chloroform. The polymer was recovered from the chloroform fraction, and the fraction is then precipitated into methanol to afford the product of dark blue solid (0.14 g, 56%). ^{1}H NMR (300 MHz, $CDCl_3$): δ (ppm) 9.01 (br, 1H), 7.64 (br, 4H), 4.14 (br, 2H), 2.00 (br, 3H), 1.42 (br, 9H), 0.94 (br, 22H).

Polymerization of PBCDPP2T

PBCDPP2T was synthesized by following the same procedure as used in the synthesis of PFDPP2T. Monomer **BC** (0.11 g, 0.19 mmol) and **DPP2T-Bo** (0.15 g, 0.19 mmol) were used as monomers, and a dark green solid was obtained as a product (0.12 g, 50%). ^{1}H NMR (300 MHz, $CDCl_3$): δ (ppm) 9.09 (br, 1H), 7.39 (br, 4H), 4.01 (br, 2H), 1.96 (br, 4H), 1.24 (br, 38H).

Fabrication of photovoltaic cells

The configuration of the solar cell device used in this work is glass/ITO/PEDOT:PSS/active layer/Ca/Al. The ITO-coated glass was cleaned with acetone and isopropyl alcohol. After complete drying at 150 ºC for 30 min, the ITO-coated glass was treated with UV–ozone for 15 min. PEDOT:PSS (Clevious AI 4083) was spin-coated on the ITO glass at 4000 rpm for 1 min and annealed at 120 ºC for 30 min to obtain a 40 nm thick film. Then, the active layer solution was spin coated onto the PEDOT:PSS-coated ITO glass. After the active layer was dried completely, Ca (20 nm) and Al (100 nm) were thermally deposited as the cathode under 3×10^{-6} Torr. The current density–voltage (J–V) characteristics were measured by a Keithley 4200 source-meter under AM 1.5 G (100 mW/cm^2) simulated by a Newport-Oriel solar simulator. The photovoltaic properties are reported on average values of 8 devices. The light intensity was calibrated using a NREL certified photodiode and light source meter prior to each measurement. The IPCE was measured using a lock-in amplifier with a current preamplifier under a short circuit current state with illumination of monochromatic light.

Characterization and measurement

The chemical structures of compounds were identified by ^{1}H NMR (Avance DPX-300) and ^{13}C NMR (Avance DPX-500). The molecular weights were measured by size exclusion chromatography (Agilent 1200 GPC) using $CHCl_3$ as an eluent. The absorption spectra were obtained by an UV–Vis spectrophotometer (Lambda 25, Perkin Elmer). Cyclic voltammetry experiments were carried out on a potentiostat/galvanostat (VMP 3, Biologic), where acetonitrile and 0.1 M tetrabutylammonium hexafluorophosphate were used as solvent and electrolyte, respectively. Platinum wires (Bioanalytical System Inc.) were used as both counter and working electrodes, and Ag/Ag^+ (Ag in 0.1 M $AgNO_3$ solution, Bioanalytical System Inc.) was used as a reference electrode. The crystallinity of active layer was investigated by a X-ray diffractometer (M18XHF-SRA, Mac Science Co.) using Cu Kα (λ=0.154 nm) radiation. GIWAXS scans were obtained at the Advanced Light Source at the Lawrence Berkeley National Laboratory. The wavelength of X-ray used was 1.240 Å, and the scattered intensity was detected by PILATUS 1M detector. The thin film morphology was observed by TEM (JEM1010) operating at 80 kV of acceleration voltage. Thickness of the active layers was measured by atomic force microscopy (Nano Xpert2).

Acknowledgements

The authors thank the Ministry of Education, Science and Technology (MEST), Korea for financial support through the Global Research Laboratory (GRL).

Notes and references

Department of Materials Science and Engineering, Seoul National University, 1 Gwanak-ro, Gwanak-gu, Seoul 151-744, Korea. E-mail: whjpoly@snu.ac.kr; Fax: +82 2-876-6086; Tel: +82 2-880-7192

† Electronic Supplementary Information (ESI) available: [Dipole moment calculation, device optimization of PBCDTBT- and PBCDPP2T-based device, $P(E,T)$ values of polymers, XRD analysis and SCLC mobilities of pure polymers]. See DOI: 10.1039/b000000x/

1 J.-C. Wang, W.-T. Weng, M.-Y. Tsai, M.-K. Lee, S.-F. Horng, T.-P. Perng, C.-C. Kei, C.-C. Yu and H.-F. Meng, *J. Mater. Chem.*, 2010, **20**, 862.
2 W. J. da Silva, H. P. Kim, A. R. bin Mohd Yusoff and J. Jang, *Nanoscale*, 2013, **5**, 9324.
3 Z. Yin, S. Sun, T. Salim, S.Wu, X. Huang, Q. He, Y. M. Lam and H. Zhang, *ACS Nano*, 2010, **4**, 5263.
4 R. R. Søndergaard, M. Hösel and F. C. Krebs, *J. Polym. Sci. Part. B: Polym. Phys*., 2013, **51**, 16.
5 N. Espinosa, M. Hösel, M. Jørgensen and F. C. Krebs, *Energy Environ. Sci*., 2014, **7**, 855.
6 Z. He, C. Zhong, S. Su, M. Xu, H. Wu, and Y. Cao, *Nature Photon*., 2012, **6**, 591.
7 S. Woo, W. H. Kim, H. Kim, Y. Yi, H.-K. Lyu and Y. Kim, *Adv. Energy Mater*. 2014, DOI: 10. 1002/aenm.201301692.
8 S.-G. Ihn, Y. Lim, S. Yun, I. Park, J. H. park, Y. Chung, X. Bulliard, J. Chang, H. Choi, J. H. Park, Y. S. Choi, G.-S. Park and H. Chang, *J. Mater. Chem. A*, 2014, **2**, 2033.
9 M. Zhang, Y. Gu, X. Guo, F. Liu, S. Zhang, L. Huo, T. P. Russell and J. Hou, *Adv. Mater*., 2013, **25**, 4944.
10 Z. He, C. Zhong, X. Huang, W.-Y. Wong, H. Wu, L. Chen, S. Su and Y. Cao, *Adv. Mater*., 2011, **23**, 4636.
11 C. Cabanetos, A. E. Labban, J. A. Bartelt, J. D. Douglas, W. R. Mateker, J. M. J. Fréchet, M. D. McGehee and P. M. Beaujuge, *J. Am. Chem. Soc*., 2013, **135**, 4656.
12 J. W. Jung, F. Liu, T. P. Rusell and W. H. Jo, *Energy Environ. Sci*., 2013, **6**, 3301.
13 J. Li, K.-H. Ong, S.-L. Lin, G.-M. Ng, H.-S. Tan and Z.-K. Chen, *Chem. Commun*., 2011, **47**, 9480.
14 C. B. Nielsen, R. S. Ashraf, B. C. Schroeder, P. D'Angelo, S. E. Watkins, K. Song, T. D. Anthopoulos and I. McCulloch, *Chem. Commun.*, 2012, **48**, 5832.
15 W. W. H. Wong, J. Subbiah, S. R. Puniredd, W. Pisula, D. J. Jones and A. B. Holmes, *Polymer. Chem*., 2014, **5**, 1258.
16 Y. Huang, M. Zhang, H. Chen, F. Wu, Z. Cao, L. Zhang and S. Tan, *J. Mater. Chem. A*, 2014, **2**, 5218.
17 B. Carsten, J. M. Szarko, H. J. Son, W. Wang, L. Lu, F. He, B. S. Rolczynski, S. J. Lou, L. X. Chen and L. Yu, *J. Am. Chem. Soc*., 2011, **133**, 20468.
18 B. Carsten, J. M. Szarko, L. Lu, H. J. Son, F. He, Y. Y. Botros, L. X. Chen and L. Yu, *Macromolecules*, 2012, 4**5**, 6390.
19 A. C. Stuart, J. R. Tumbleston, H. Zhou, W. Li, S. Liu, H. Ade and W. You, *J. Am. Chem. Soc*., 2013, **135**, 1806.
20 Z. Xiao, J. Subbiah, K. Sun, S. Ji, D. J. Jones, A. B. Holmes and W. W. H. Wong, *J. Mater. Chem. C*, 2014, **2**, 1306.
21 E. H. Jung and W. H. Jo, *Energy Environ. Sci*., 2014, **7**, 650.
22 J. W. Jung, F. Liu, T. P. Russell and W. H. Jo, *Energy Environ. Sci*., 2012, **5**, 6857.
23 M. Shahid, R. S. Ashraf, Z. Huang, A. J. Kronemeijer, T. McCarthy-Ward, I. McCulloch, J. R. Durrant, H. Sirringhaus and M. Heeney, *J. Mater. Chem.*, 2012, **22**, 12817.
24 P. Sonar, S. P. Shingh, Y. Li, Z.-E. Ooi, T.-J. Ha, I. Wong, M. S. Soh and A. Dodabalapur, *Energy Environ. Sci*., 2011, **4**, 2288.
25 C. J. Barbec, A. Cravino, D. Meissner, M. S. Sariciftci, T. Fromherz, M. T. Rispens, L. Sanchez and J. C. Hummelen, *Adv. Funct. Mater*., 2001, **11**, 374.
26 Y.-J. Cheng, S.-H Yang and C.-S. Hsu, *Chem. Rev*., 2009, **109**, 5868.
27 J. C. Bijleveld, V. S. Gevaerts, D. D. Nuzzo, M. Turbiez, S. G. J. Mathijssen, D. M. de Leeuw, M. M. Wienk and R. A. J. Janssen, *Adv. Mater*., 2010, **22**, E242.
28 W. Li, A. Furlan, W. S. C. Roelofs, K. H. Hendriks, G. W. P. van Pruissen, M. M. Wienk and R. A. J. Janssen, *Chem. Commun.*, 2014, **50**, 679.
29 J. W. Jung, J. W. Jo, F. Liu, T. P. Russell and W. H. Jo, *Chem. Commun.*, 2012, **48**, 6933.
30 N. Blouin, A. Michaud and M. Leclerc, *Adv. Mater*., 2007, **19**, 2295.
31 S. H. park, A. Roy, S. Beaupré, S. Cho, N. Coates, J. S. Moon, D. Moses, M. Leclerc, K. Lee and A. J. Heeger, *Nature Photon*., 2009, **3**, 297.
32 M. Ide, Y. Koizumi, A. Saeki, Y. Izumiya, H. Ohkita, S. Ito and S. Seki, *J. Phys. Chem. C*, 2013, **117**, 26859.
33 S. Li, Z.Yuan, P. Deng, B. Sun and Q. Zhang, *Polym. Chem.*, 2014, **5**, 2561.
34 O. Inganäs, M. Svensson, F. Zhang, A. Gadisa, N. K. Persson, X. Wang and M. R. Andersson, *Appl. Phys. A*, 2004, **79**, 31.
35 M.-H. Chen, J. Hou, Z. Hong, G. Yang, S. Sista, L.-M. Chen and Y. Yang, *Adv. Mater*., 2009, **21**, 4238.
36 L. H. Slooff, S. C. Veenstra, J. M. Kroon, D. J. D. Moet, J. Sweelssen and M. M. Koetase, *Appl. Phys. Lett.*, 2007, **90**, 143506.
37 A. P. Zoombelt, S. G. J. Mathijssen, M. G. R.Turbiez, M. M. Wienk and R. A. J. Janssen, *J. Mater. Chem.*, 2010, **20**, 2240.
38 D. Mühlbacher, M. Scharber, M. Morana, Z. Zhu, D. Waller, R. Gaudiana and C. Barbec, *Adv. Mater*., 2006, **18**, 2884.
39 A. P. Zoombelt, M. Fonrodona, M. G. R. Turbiez, M. M. Wienk and R. A. J. Janssen, *J. Mater. Chem.*, 2009, **19**, 5336.
40 L. Dou, C.-C. Chen, K. Yoshimura, K. Ohya, W.-H. Chang, J. Gao, Y. Liu, E. Richard and Y. Yang, *Macromolecules*, 2013, **46**, 3384.
41 C. Müller, E. Wang, L. M. Andersson, K. Tvingstedt, Y. Zhou, M. R. Andersson and O. Inganäs, *Adv. Funct. Mater*., 2010, **20**, 2124.
42 W. Ma, C. Yang and A. J. Heeger, *Adv. Mater*., 2007, **19**, 1387.
43 J.-L. Wu, F.-C. Chen, Y.-S. Hsiao, F.-C. Chien, P. Chen, C.-H. Kuo, M. H. Huang and C.-S. Hsu, *ACS Nano*, 2011, **5**, 959.
44 L. Lu, Z. Luo, T. Xu and L. Yu, *Nano Lett.*, 2013, **13**, 59.
45 V. D. Mihailetchi, L. J. A. Koster, J. C. Hummelen and P. W. M. Blom, *Phys. Rev. Lett.*, 2004, **93**, 216601.
46 J. Liu, H. Choi, J. Y. Kim, C. Bailey, M. Durstock and L. Dai, *Adv. Mater*., 2012, **24**, 538.
47 B. Fu, J. Baltazar, Z. Hu, A.-T. Chien, S. Kumar, C. L. Henderson, D. M. Collard and E. Reichmanis, *Chem. Mater.*, 2012, **24**, 4123.
48 C. Kanimozhi, N. Yaacobi-Gross, K. W. Chou, A. Amassian, T. D. Anthopoulos and S. Patil, *J. Am. Chem. Soc*., 2012, **134**, 16532.

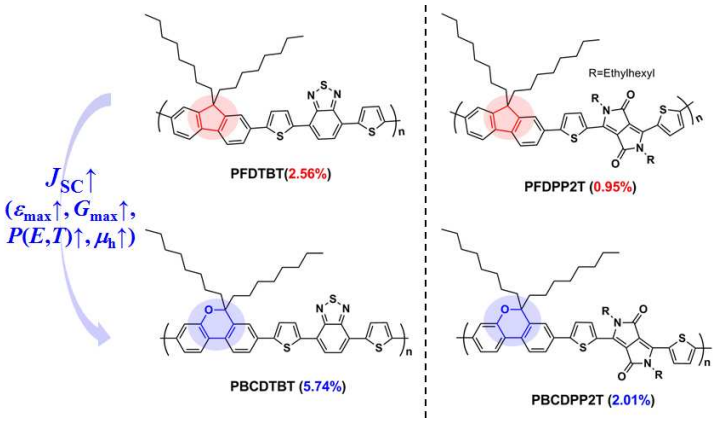

PBCDTBT and PBCDPP2T are synthesized by introducing an oxygen atom in fluorene unit in PFDTBT and PFDPP2T, respectively. PBCDTBT- and PBCDPP2T-based devices exhibit higher J_{SC}s than those of PFDTBT and PFDPP2T-based devices, respectively, due to stronger and broader light absorption, higher exciton generation rate, more effective charge separation and higher hole mobility.